

A FRAMEWORK FOR PARAMETERS ESTIMATION OF IMAGE OPERATOR CHAIN

Xin Liao*, Zihang Huang

College of Computer Science and Electronic Engineering, Hunan University, Changsha 410082, China.

ABSTRACT

Currently, many effective techniques have been proposed to estimate the parameters of tampering operations. Most of them consider the situation that an image is tampered by only one operation. However, multiple manipulation operations are always used to tamper an image in our daily life. Moreover, since the tampering traces of previous operations may be weakened or eliminated by later ones, the detecting accuracy of methods used for detecting single operations would be reduced. In this paper, we propose a new method to estimate the parameters of operations in different manipulation chains. Especially, we first investigate the correlation of operations and divide the degree of interactions between them into uncoupled and coupled. Furthermore, resizing and median filtering are adopted to reveal the assessment framework. Meanwhile, we propose well-directed features including energy density of difference-image to estimate operation parameters. The experiment proves the effectiveness of our method.

Index Terms— Image forensics, operator chains, parameters estimation, coupled operations, uncoupled operations

1. INTRODUCTION

Nowadays, digital multimedia plays an important role in people's daily life. However, with the rapid development of media editing software, digital multimedia contents can be easily manipulated [1]. In recent years, many state-of-the-art image forensic techniques have been proposed to detect the types of tampering operations that multimedia images have gone through, such as median filtering [2], contrast enhancement [3], resizing [4], blurring [5] and copy-move [6]. Furthermore, some universal forensic techniques have been proposed to detect various types of manipulation operations [7, 8]. However, these above methods only focus on identifying the existence of a single operation in the presence of manipulation chains. Considering multiple operations are always used to tamper images and different operation topologies have distinct influences on images, many novel methods are adopted to detect operations in operator chains. The concept of operator chain forensics was first proposed in [9, 10], and the

authors theoretically analyzed the possibility of using single operation tampering forensics algorithms to detect image manipulation chain. In our previous work [11], the sudden gaps and zeros in the histogram and a new adaptive window cutoff function are used to detect the order of contrast enhancement and resizing.

Moreover, in order to obtain more precise detection results, some methods are investigated to estimate the parameters of tampering operations. The authors in [12] proposed a new method to estimate the parameters of resampling according to the variations of energy in the image's frequency domain. Inspired by this, Zhu et al. [13] adopted a new method named learning-to-rank to automatically achieve the estimation of the scaling factor.

However, to the best of our knowledge, no work involves the situation estimating the parameters of operator chains. Distinct combinations of tampering operations will produce confusion processing effects in operator chains. The digital features designed for estimating the parameters of specific operations would be weakened or even eliminated. Therefore, we need to investigate whether there exists interaction between the tampering operations.

In this paper, we propose a novel method to estimate the parameters of multiple tampered images based on analyzing the interaction degree of multiple operations. To begin with, we exploit the inherent connection among image pixels to investigate the interaction of multiple tampering operations. According to the effects of topologies and operation parameters on tampered images, we divide the interaction degree into uncoupled and coupled. To validate the correctness of our work, the proposed method is applied to detecting resizing and median filtering.

2. THE INTERACTION DEGREE OF TAMPERING OPERATIONS IN OPERATOR CHAINS

In the process of image manipulation, various operations might make image pixels be a combination of their neighbors that will introduce periodic correlations among them. Therefore, different operations will influence each other more or less, which may decrease the accuracy of estimating parameters. To estimate parameters more accurately, from the perspective of topologies and operation parameters, we further analyze the interaction degree between distinct operations.

*Corresponding author: xinliao@hnu.edu.cn

This work is supported by National Natural Science Foundation of China (Nos. 61972142, 61972143, 61972395, 61772191), Open Project Program of National Laboratory of Pattern Recognition (No. 201900017).

Assume there are n different operations contained in a tampering chain are denoted as $O = (o_1, o_2, \dots, o_n)$. Therefore, $S = (S_1, S_2, \dots, S_{Num(S)})$ is the set of operator chains generated by combining these operations in any order. Here, $Num(S) = A_n^n$ denotes the number of different operator chains and A is the symbol of permutation. Then, we use I_{S_j} to denote the tampered image that experienced a specific operator chain S_j . According to the relation of tampered images, we propose the first definition of the discriminant criterion:

Definition 1. *If operations are uncoupled, the tampered image should satisfy the following condition*

$$I_{S_1} = I_{S_2} = \dots = I_{S_{Num(S)}} \quad (1)$$

This definition indicates that exchanging the order of multiple operations will not produce any difference in the final generated image.

Since the extraction of digital features is the main step in parameter estimation, the influence of operation parameters on digital features is important to measure whether operations are uncoupled. From the perspective of operation parameters, we further exploit the tampering traces left by different operations. For a specific operator chain S_j , we analyze the influence of the changes of operation parameters on the image. Let $\bigcup \theta_i$ denote the range of parameters of operation o_i such as

$$\bigcup \theta_i = \{\theta_i^l, \theta_i^2, \dots, \theta_i^{z_i}\} \quad (2)$$

where θ_i^l is the smallest parameter of operation o_i , and $\theta_i^{z_i}$ is the largest one. Therefore, the operator chain is

$$S_j(x_1, x_2, \dots, x_n), x_i \in \bigcup \theta_i \quad (3)$$

where x_i denote the operation o_i and its parameters. Then, we construct a function $f_{o_i}(\cdot)$ to represent the specific detecting feature for operation o_i . According to the influence of operation parameters on digital features, we give the second definition of discriminant criterion:

Definition 2. *If operations are coupled, the result of function $f_{o_i}(\cdot)$ will be affected by the changes in the parameters of other operations, i.e.,*

$$|f_{o_i}(I_{S_j}(x_1, \dots, x_i, \dots, x_n)) - f_{o_i}(I_{S_j}(\bar{x}_1, \dots, x_i, \dots, \bar{x}_n))| \neq 0 \quad (4)$$

where $I_{S_j}(x_1, \dots, x_i, \dots, x_n)$ represents the tampering operator chain S_j including one specific operation o_i and other operations. x and \bar{x} represent the same operation with different parameters. If the tampering operations satisfy Eq. (4), we can claim that these operations are coupled.

Our framework is shown in Fig. 1. If the operations are uncoupled, the parameters can be separately estimated by adopting existing methods used for detecting single operations. If the operations are coupled, we need to construct new features of each operation to estimate the parameters, and consider the order of multiple operations.

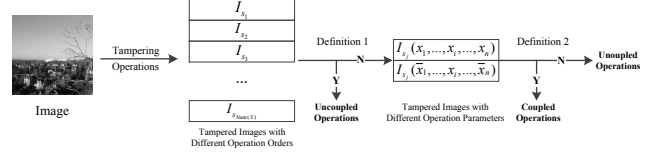


Fig. 1. The framework of distinguishing the interaction degree between multiple operations.

3. ESTIMATING THE PARAMETERS OF RESIZING AND MEDIAN FILTERING

In this section, we use specific tampering operations to clarify the framework of distinguishing the interaction degree between multiple operations.

3.1. Analysis the Interaction between Resizing and Median Filtering

Median filtering is a nonlinear smoothing operation that turns the current pixel into the median value of its correlation window. In the interpolation process of resizing operation, the inserted pixels are related to their surrounding pixels. Here, I_{S_1} denotes the tampered image experienced median filtering then resizing and I_{S_2} denotes the reverse order. At first, we describe an original image experienced median filtering then resizing. In order to simplify the description process, we only discuss the linear interpolation in the horizontal direction with the ratio more than 1 and the window size of median filtering is 3×3 . For the original image $P = (p_{ij})^{n \times n}$, the pixel $M(i, j)$ in the median filtered image is

$$M(i, j) = m(p(i, j)) \quad (5)$$

where $m(\cdot)$ is the process of selecting the median value of one pixel's correlation window. After the interpolation process, the final tampered image I_{S_1} is

$$I_{S_1} = \begin{bmatrix} M(1, 1) & N(1, 1) & \dots & M(1, 2) & \dots \\ \vdots & \vdots & \vdots & \ddots & \vdots \\ M(n, 1) & N(n, 1) & \dots & M(n, 2) & \dots \end{bmatrix} \quad (6)$$

where $N(i, j)$ is newly generated pixel. For linear interpolation, these pixels are related to their adjacent original pixels. Next, we discuss the first column of them

$$N(i, 1) = \alpha M(i, 1) + \beta M(i, 2) \quad (7)$$

where α and β are the weights of different resizing factors.

If we adjust the order of operations, resize the original image P first, the first column of newly generated pixels is

$$R(i, 1) = \alpha p(i, 1) + \beta p(i, 2) \quad (8)$$

Then, after median filtering, we find the $R(i, 1)$ is changed to

$$\tilde{N}(i, 1) = m(R(i, 1)) \quad (9)$$

According to Eq. 5 and Eq. 7, the newly generated pixel $N(i, 1)$ can be expressed as

$$N(i, 1) = \alpha m(p(i, 1)) + \beta m(p(i, 2)) \quad (10)$$

In a similar way, Eq. 9 could be converted into

$$\tilde{N}(i, 1) = m(R(i, 1)) = m(\alpha p(i, 1) + \beta p(i, 2)) \quad (11)$$

Since interpolation process will introduce new pixels in the fixed window of median filtering and $m(\cdot)$ is a nonlinear operation, $N(i, 1)$ and $\tilde{N}(i, 1)$ could hardly be equal based on natural images. Therefore, two tampered images are different (i.e. $I_{S_1} \neq I_{S_2}$), and they do not satisfy Definition 1.

As shown in Fig. 2, two histograms of the images tampered by different operation orders are distinct. Therefore, there exists difference between two tampered images in spatial domain, which accords with the above statement.

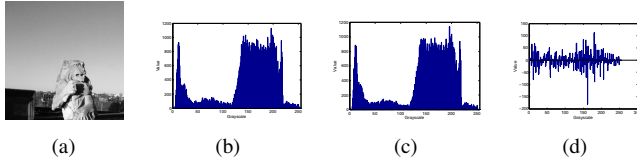


Fig. 2. Histograms of tampered images. (a) the original image. (b) image that experienced resizing before median filtering. (c) image that experienced median filtering before resizing. (d) the difference of two histograms.

Because Definition 1 is not satisfied, according to our proposed framework, we need to determine the interaction degree of two operations following by Definition 2. In [12] a novel energy-based method was proposed to estimate the parameters of resizing. The energy E can be expressed as

$$E = \sum_{x=1}^n \sum_{y=1}^n p(i, j)^2 = \sum_{u=-\omega}^{\omega} \sum_{v=-\omega}^{\omega} |p(u, v)|^2 \quad (12)$$

where ω is the cutoff frequency of the image, $p(u, v)$ is the frequency spectrum. Then, we assume that the ratio of the energy between the high-frequency part and the whole image after applied median filtering is

$$\frac{E_{\omega_c}}{E_{\omega}} = \frac{\sum_{u=-\omega_c}^{\omega_c} \sum_{v=-\omega_c}^{\omega_c} |p(u, v)|^2}{\sum_{u=-\omega}^{\omega} \sum_{v=-\omega}^{\omega} |p(u, v)|^2} = a \quad (13)$$

It is known that median filtering with the larger window size would result in the smoother image. If we adjust the window size of median filtering, the ration between high-frequency part and the whole image would become to

$$\frac{E'_{\omega_c}}{E'_{\omega}} = \frac{\sum_{u=-\omega_c}^{\omega_c} \sum_{v=-\omega_c}^{\omega_c} |p'(u, v)|^2}{\sum_{u=-\omega}^{\omega} \sum_{v=-\omega}^{\omega} |p'(u, v)|^2} = k \times a \quad (14)$$

where $k \neq 1$. Overall, in our method, we can calculate the value of $\left(\left|\frac{E_{\omega_c}}{E_{\omega}}\right| - \left|\frac{E'_{\omega_c}}{E'_{\omega}}\right|\right) = (1 - k) \times a \neq 0$. The features designed for detecting resizing is affected by the window size of median filtering. Therefore, Definition 2 is satisfied, and then resizing and median filtering are coupled.

3.2. The Estimation Feature of Resizing and Median Filtering

Median filtering will weak the periodic artifacts introduced by resizing, and the traces of them will be covered up by each other. Therefore, we improve the normalized energy density method [12] by extending the feature dimension and highlighting the feature difference of different parameters to estimate two factors. The feature can be expressed as:

$$E_n(w) = \frac{\sum |\hat{p}(u, v)|^2}{w^2 \sum |p(u, v)|^2} \quad (15)$$

where $w \in (0, 1]$ is the window size, $\sum \hat{p}(u, v)$ and $\sum p(u, v)$ are the sum of frequency spectrum value of the selected area and the whole image, respectively.

Difference-image can highlight the details of image texture and the distribution can be expressed by the generalized Gaussian distribution. Here, the difference-image is

$$\begin{cases} p_x(i, j) = p(i+1, j) - p(i, j), i, j = 1, 2, \dots, n-1 \\ p_x(n, j) = p(n, j) \end{cases} \quad (16)$$

$$\begin{cases} p_y(i, j) = p(i, j+1) - p(i, j), i, j = 1, 2, \dots, n-1 \\ p_y(i, n) = p(i, n) \end{cases} \quad (17)$$

where $p_x(i, j)$ and $p_y(i, j)$ are the pixel values of difference image in the vertical and horizontal direction, respectively.

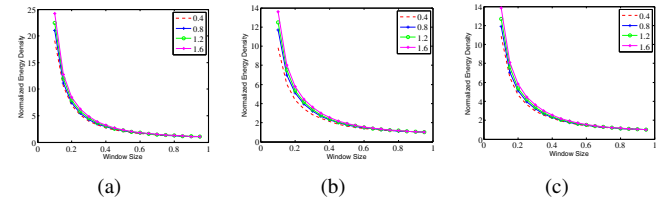


Fig. 3. The average normalized energy densities of 1000 tampered images. (a) gray image. (b) difference-image in vertical direction. (c) difference-image in horizontal direction.

Before calculating the normalized energy density, we need to reduce the strong low-frequency components in the spectrum. In our method, the Laplacian filter which is the two-dimensional discrete approximation of Laplacian operators is used to highlight the high-frequency portion of digital images. Specially, we use the filter with kernel K as below

$$K = \begin{bmatrix} 0 & -1 & 0 \\ -1 & 4 & -1 \\ 0 & -1 & 0 \end{bmatrix} \quad (18)$$

Fig. 3 shows the energy-based feature of 1000 tampered images experienced resizing then median filtering with different resizing factors (0.4, 0.8, 1.2, 1.6) and the median filtering parameter is 5×5 . The window size of the normalized energy density method is in the range $[0.1, 0.95]$ with the step of 0.05. In the original image and difference-image, it is shown

Table 1. Comparison results (%) of our proposed method and Feng et al. [12] for estimating the parameters of resizing and median filtering applied on images.

Parameters		0.4		0.6		0.8		1		1.2		1.4		1.6		1.8	
Order	Size	Ours	[12]	Ours	[12]	Ours	[12]	Ours	[12]	Ours	[12]	Ours	[12]	Ours	[12]	Ours	[12]
RS-MF	3×3	91.0	88.0	89.6	76.3	90.6	78.2	84.7	83.6	83.2	76.4	74.8	64.3	91.8	86.6	76.5	67.5
	5×5	90.7	87.0	88.1	76.3	90.4	76.9	82.2	71.2	82.2	75.4	75.5	62.1	93.2	89.5	80.8	70.2
	7×7	81.2	77.0	90.4	78.0	91.4	83.9	86.3	74.4	84.3	78.2	72.9	64.8	93.6	89.9	73.5	61.8
MF-RS	3×3	87.2	87.4	90.8	86.2	91.0	87.5	90.7	78.8	89.2	78.2	89.4	77.3	90.2	80.5	91.5	78.7
	5×5	84.0	87.0	91.5	85.8	90.7	87.2	88.8	78.0	87.1	76.0	88.5	77.6	91.0	79.2	90.0	80.9
	7×7	86.5	82.5	89.0	80.6	91.1	84.5	91.0	79.7	90.2	78.8	90.7	77.6	90.6	80.2	93.7	76.4

Table 2. Comparison results (%) of our proposed method and Feng et al. [12] for estimating the parameters of resizing and median filtering applied on JPEG images.

Parameters		0.4		0.6		0.8		1		1.2		1.4		1.6		1.8	
Order	Size	Ours	[12]	Ours	[12]	Ours	[12]	Ours	[12]	Ours	[12]	Ours	[12]	Ours	[12]	Ours	[12]
RS-MF	3×3	93.9	83.0	92.7	78.2	96.2	82.6	83.8	79.1	86.7	82.1	82.2	77.3	91.5	93.3	88.1	89.9
	5×5	91.9	83.7	89.3	79.3	91.2	81.5	83.5	76.3	83.1	78.2	72.6	64.2	91.7	86.9	78.0	70.4
	7×7	88.1	74.4	89.4	72.8	91.6	79.5	85.2	68.9	87.1	76.5	71.7	60.6	94.6	91.8	77.7	63.0
MF-RS	3×3	82.8	81.9	89.5	87.7	94.9	90.7	89.0	82.4	89.9	83.6	86.9	77.7	92.5	86.4	89.9	83.9
	5×5	81.9	75.8	89.5	87.0	92.1	88.1	90.4	82.8	87.4	77	86.6	76.9	91.8	81.4	86.9	81.4
	7×7	86.5	83.5	91.1	84.0	93.1	84.9	90.6	73.2	88.4	77.6	90.6	78.1	92.7	82.5	87.8	77.9

that for different operation parameters, the curves of normalized energy density feature are distinct. Thus, we could use this energy-based feature in the original image and difference-image to form a multi-dimensional feature, so as to estimate the parameters of resizing and median filtering.

4. EXPERIMENTAL RESULTS

In this section, we show the performance of our method for estimating the parameters of median filtering and resizing.

4.1. Experimental Settings

In the experiment, two image data sets are used to form the training set and the test set. Especially, we use BOSS database [14] which contains 10000 images as a training set and use UCID database [15] as a test set. To obtain enough images, we cut the images from BOSS database to the size of 256×256 by the diagonal line. Similarly, we crop the images from UCID database by selecting their 256×256 central parts. The proposed energy-based feature is used as input to train multi-class SVM classifiers with polynomial kernel.

4.2. Performance in Parameters Estimation of Median Filtering and Resizing

In this part, we detect median filtering and resizing with different parameters. The window size of median filtering includes 3×3 , 5×5 and 7×7 . The parameter of resizing ranges from 0.4 to 1.8 in steps of 0.2.

Because median filtering and resizing are coupled, we train two classifiers for different image operation orders. We

tamper 1000 images from BOSS database with each parameter of median filtering and resizing. Meanwhile, 1000 UCID images are similarly tampered with each pair of parameters.

Table 1 shows the accuracy rates for detecting images tampered by resizing with factors from 0.4 to 1.8 and median filtering with different window sizes. RS-MF represents images experience resizing then median filtering, MF-RS represents the reverse order. Our work is effective and the estimation performance is greater than the method mentioned in [12]. The average accuracy rates are increased by near 10%. Furthermore, Table 2 presents the performance for detecting JPEG images. Our proposed method could improve the average accuracy rates by more than 8%.

5. CONCLUSION

In this paper, a new method is proposed to estimate the operation parameters in operator chains. Firstly, by investigating the inherent correlation among different tampering operations from the perspective of topologies and operations parameters, we divide the interaction degree of operations into coupled and uncoupled. Then, based on the interaction degree of multiple operations, the well-directed features are proposed. Specifically, the normalized energy density of difference image is adopted to detect their parameters. Our future work contains extending the number of operations to more than two. As the number of operations increases, the interaction among operations may change. Therefore, more complex interaction among different manipulations would be considered.

6. REFERENCES

- [1] Stamm M. C., Wu M., Liu K. J. R., Information forensics: an overview of the first decade, *IEEE Access*, 2013, pp. 167-200.
- [2] Chen C., Ni J., Huang J., Blind detection of median filtering in digital images: A difference domain based approach, *IEEE Transactions on Image Processing*, 2013, 22(12), pp. 4699-4710.
- [3] Singh N., Gupta A., Jain R., Global contrast enhancement based image forensics using statistical features, *Advances in Electrical and Electronic Engineering*, 2017, 15(3), pp. 509-516.
- [4] Popescu A., Farid H., Exposing digital forgeries by detecting traces of resampling, *IEEE Transactions on Signal Processing*, 2008, 53(2), pp. 758-767.
- [5] Su B., Lu S., Tan C., Blurred image region detection and classification, *ACM International Conference on Multimedia*, 2011, pp. 1397-1400.
- [6] Li J., Li X., Yang B., Sun X., Segmentation-based image copy-move forgery detection scheme, *IEEE Transactions on Information Forensics and Security*, 2015, 10(3), pp. 507-518.
- [7] Qiu X., Li H., Luo W., Huang J., A universal image forensic strategy based on steganalytic model, *ACM Workshop on Information Hiding and Multimedia Security*, 2014, pp. 165-170.
- [8] Li H., Luo W., Huang J., Identification of various image operations using residual-based features, *IEEE Transactions on Circuits and Systems for Video Technology*, 2018, 28(1), pp. 31-45.
- [9] Comesaña P., Detection information theoretic measures for quantifying the distinguishability between multimedia operator chains, *IEEE International Workshop on Information Forensics and Security*, 2012, pp. 211-216.
- [10] Comesaña P., Pérez-González F., Multimedia operator chain topology and ordering estimation based on detection and information theoretic tools, *International Conference on Digital Forensics and Watermarking*, 2013, pp. 213-227.
- [11] Gao S., Liao X., Guo S., Forensic detection for image operation order: resizing and contrast enhancement, *International Conference on Security, Privacy and Anonymity in Computation, Communication and Storage*, 2017, pp. 570-580.
- [12] Feng X., Cox I., Doerr G., Normalized energy density-based forensic detection of resampled images, *IEEE Transactions on Multimedia*, 2012, 14(3), pp. 536-545.
- [13] Zhu N., Deng C., Gao X., A learning-to-rank approach for image scaling factor estimation, *Neurocomputing*, 2016, 204, pp. 33-40.
- [14] Patrick B., Filler T., Pevný, T., Break our steganographic system: the ins and outs of organizing BOSS, *International Workshop on Information Hiding*, 2011, pp. 59-70.
- [15] Schaefer G., Stich M., UCID: an uncompressed color image database, *SPIE, Storage and Retrieval Methods and Applications for Multimedia*, 2004, pp. 472-480.